Supporting Information

Integrative toxicoproteomics implicates impaired mitochondrial glutathione import as off-target effect of troglitazone

Yie Hou Lee,[1,†,*] Wilson Wen Bin Goh,[2] Choon Keow Ng,[3] Manfred Raida,[1,3] Limsoon Wong,[4,5] Qingsong Lin [6] Urs A. Boelsterli,[7] and Maxey C.M. Chung[1,6,*]

*From the [1]Department of Biochemistry, Yong Loo Lin School of Medicine, National University of Singapore, Singapore; [2]Department of Computing, Imperial College, London; [3]Experimental Therapeutics Centre, A*STAR, Singapore; [4]School of Computing, [5]Department of Pathology, [6]Department of Biological Sciences, Faculty of Science, National University of Singapore, Singapore; [7]Department of Pharmaceutical Sciences, School of Pharmacy, University of Connecticut, Storrs, CT, USA*

Running title: Integrative toxicoproteomics of troglitazone

[†]Current address: *Biosystems and Micromechanics, and Infectious Diseases Inter-disciplinary Research Groups*, *Singapore MIT Alliance for Research and Technology, Singapore*

***Address for correspondence/proofs:**

Maxey C.M. Chung, PhD

Department of Biochemistry, Yong Loo Lin School of Medicine, National University of Singapore, Singapore

MD7, 8 Medical Drive, Singapore 117597

Email: maxey_chung@nuhs.edu.sg; Phone: +65-6516-3252; Fax: +65-779-1453

OR

Yie Hou Lee, PhD

Biosystems and Micromechanics, and Infectious Diseases Inter-disciplinary Research Groups, Singapore-MIT Alliance for Research and Technology, Singapore

1 CREATE Way, #04-13/14 Enterprise Wing, Singapore 138602

Email: yie.hou@smart.mit.edu; Phone: +65-6601 1694; Fax: 6684 2118

Supplementary Figure 1. iTRAQ analysis of mouse hepatic mitoproteome. (A) Graph showing the more conservative "instantaneous" FDR against the more commonly used and liberal "aggregate" FDR in limiting false positives. (B) Histogram of mean signal area (intensity) of reporter channels of the 4-plex and 8-plex system. They were binned according to percentiles. The 5th percentile was disregarded for its poorer ion statistics; thereafter percentiles were taken as denoted by red arrow.

Supplementary Figure 2. Validation of MS detected mitochondrial proteins. (A) Immunoblotting and (B) MRM demonstrate accuracy of mass-spectrometry results. (C) Silver stained 1D gel of *Sod2*$^{+/+}$ and *Sod2*$^{+/-}$ liver mitochondrial proteins serves as normalization control for immunoblotting.

Supplementary Figure 3. *Sod2*$^{+/-}$ versus wildtype mouse hepatic mitoproteome and biochemical endpoints. (A) Mitochondrial GSH (mGSH), nitrotyrosine (3-NT) and protein carbonylation levels isolated from hepatic mitochondria of *Sod2*$^{+/+}$ and *Sod2*$^{+/-}$ mice. n =4 mice per genotype, Student's t-test, $P < 0.05$. (B) Pie chart of statistically significant GO overrepresented "biological processes" terms with *Sod2* haplodeficiency. Proteins for which no annotations could be assigned were excluded from the analysis for both the hits and the global set. The number of proteins assigned to each category is shown in brackets. $P < 0.01$ after Bonferroni correction for multiple testing.

Supplementary Figure 4. Proteomics of troglitazone treated *Sod2*$^{+/-}$ mitochondria. (A) Immunoblot analysis of selected mitochondrial proteins. Equal amounts of mitochondrial lysate (5 µg) were separated on SDS-PAGE, immunoblotted against their specific antibodies and their expression quantified (n = 3). Immunoblotted ratios are in agreement with MS-determined fold ratios except NDUFS3 for reasons specified in Experimental Procedures. VEH, vehicle-administered and TRG, troglitazone-administered. (B) Protein attribute evaluation of isoelectric point, molecular weight, size and hydrophobicity of detected proteins against annotated mitochondrial proteins (Pagliarini et al. 2008). Grey columns indicate annotated proteins and white columns represent detected proteins. (B) GO slim analysis of detected mitochondrial proteins demonstrates substantial representation of "Biological processes" and "Molecular functions" annotated to the mitochondrion.

Supplementary Figure 5. Functional and toxicological analysis of troglitazone-treated *Sod2*$^{+/-}$ mitoproteome. Schematic diagram showing the relationship of mitochondrial dysfunction and oxidative stress with troglitazone administration. Multiple points of elevated ROS levels (yellow) by troglitazone contributed to the up-regulation (red) and down-regulation (green) of mitochondrial proteins. The diagram shows the 28 days-weeks impact; for 14 days, the fold change are reversed.

Supplementary Figure 6. Topology dynamics of *Sod2*$^{+/-}$ hepatic mitoproteome with troglitazone exposure. (A) Expanded mitonetworks at 14 and 28 days depict proteome network transition with troglitazone administration. Expansion was based on the recovery of first degree neighbors of identified seed proteins. More seed proteins were derived in the 28 days period, and this necessarily affected a greater part of the Mitonetwork, thereby also generating a much denser and larger network. (B) The connected components at both 14 and 28 days respectively without expansion. The merged subnetwork connects both components from 14 and 28 days. There seems to be a progression change where at 14 days, seeds in the connected component corresponded to the NDUF complex and some lipid associated proteins. At 28 days, this seems to have expanded into a series of metabolic associated functions branching off from the lipid-associated proteins, and affecting processes such as apoptosis, and many other varied metabolic functions. (C) Box plots of protein expressions of proteins with and without established and predicted PPRE sequences. The outliers were based off a 95th percentile cut-off. 14 days ($median_{14\ days}$ = 1.13, Wilcoxon P < 0.01) and 28 days ($median_{28\ days}$ = 1.11 versus 1.03 respectively; Wilcoxon P = 0.1959).

Supplementary Figure 7. *Sod2* genotype and ACO2 activity and damage with troglitazone. (A) ACO2 activity with troglitazone administration in *Sod2*$^{+/-}$ liver mitochondria. Mean ± S.D. are shown. n = 3-6 per group.**P < 0.01 and $^{\#\#\#}P$ < 0.001 for 28 days troglitazone treated compared to 28 days vehicle and 14 days vehicle respectively. (B) Varying degrees of ACO2 oxidative modification after troglitazone administration. 10 µg proteins were separately loaded onto 8% non-denaturing gels and 12.5% denaturing gels and immunoprobed for ACO2. Top section denotes ACO2 aggregate formation with prolonged troglitazone treatment. Middle section shows the reduced amounts of intact ACO2 (83 kDa) with 14 and 28 days troglitazone administration due to its different modifications. The smudge of the column second from the right was probably due to non-specific staining. The bottom section shows the cleaved fragment ACO2. The lighter 40 kDa bands but increased aggregation with 28 days of troglitazone treatment suggests a continuum of ACO2 oxidative modification. Note that the total intensities of the three sections correspond well with the basal levels of ACO2 as detected in the proteomics screen. (R_{14days} ≈ 0.98 and R_{28days} ≈ 1.08). (C-E) Measurements of mitochondrial 3-NT levels (C), liver nitrate/nitrite levels (D) and cytochrome c release (E) into the cytosol of *Sod2*$^{+/-}$ after 14 and 28 days troglitazone administration. Mean ± S.D. are shown. n = 3-6 per group; 1-way ANOVA with Bonferroni post test; *P < 0.05, **P < 0.01, ***P < 0.001. VEH, vehicle-administered and TRG, troglitazone-administered. $^{\#}P$ < 0.05, $^{\#\#}P$ < 0.01 and $^{\#\#\#}P$ <0.001 for 4 weeks treated compared with 14 days vehicle; $^{\%}P$ < 0.05 and $^{\%}P$ < 0.001 for 28 days treated compared with 14 days treated; *P < 0.05 and ***P < 0.001 for 28 days treated compared with 28 days vehicle.

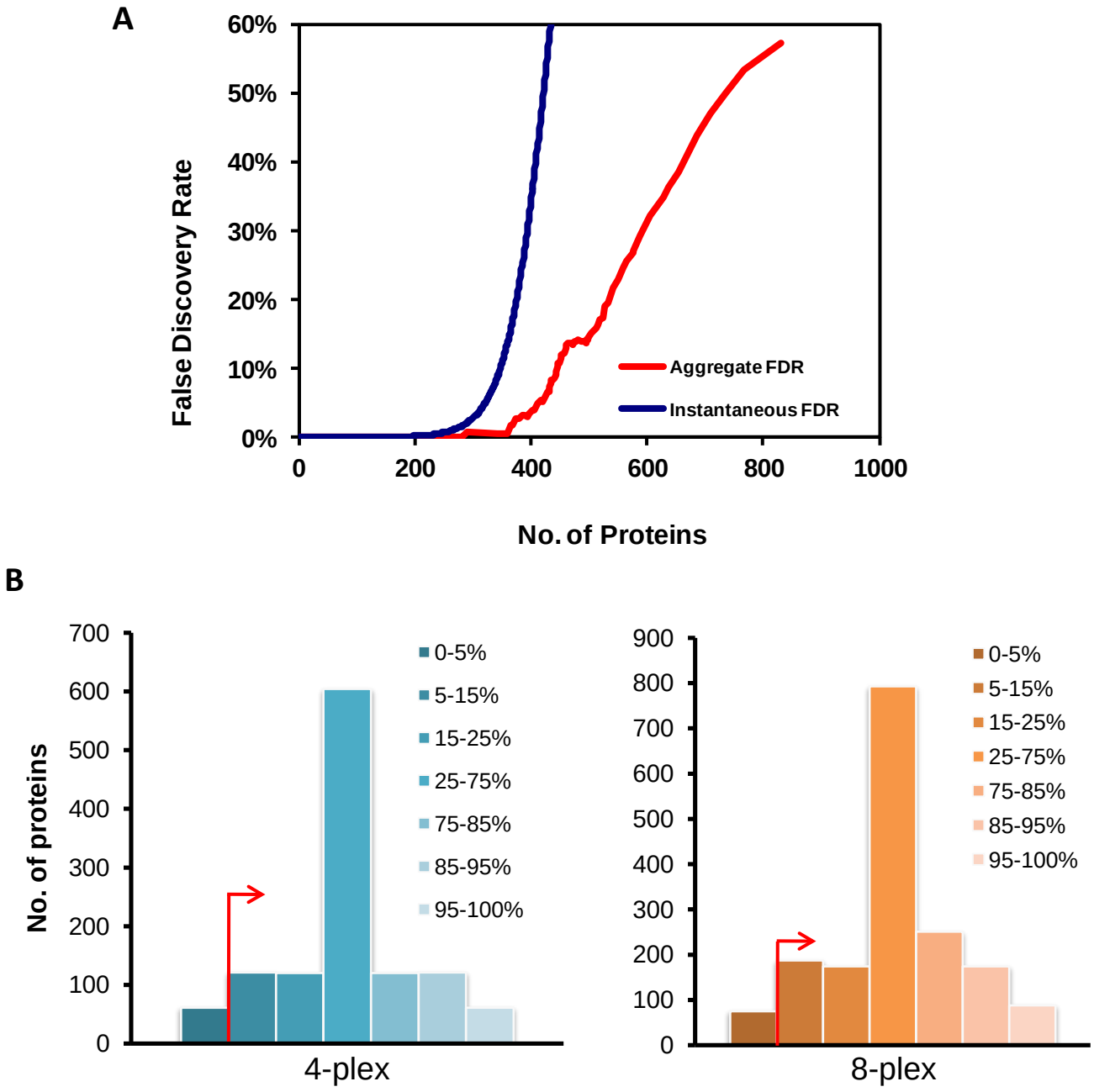

Supplementary Figure 1

A

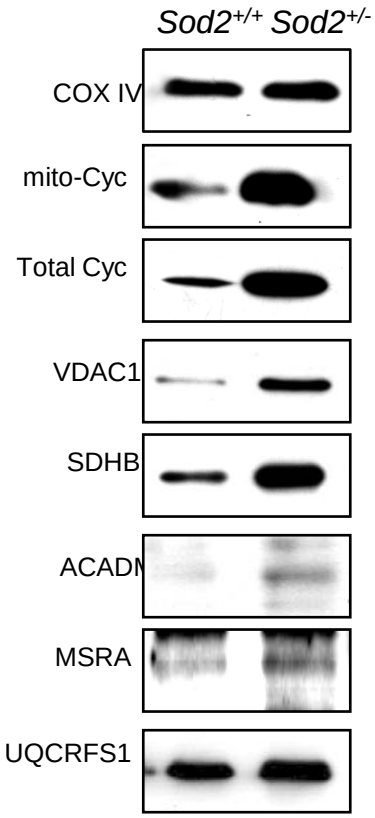

Immunblotting

B

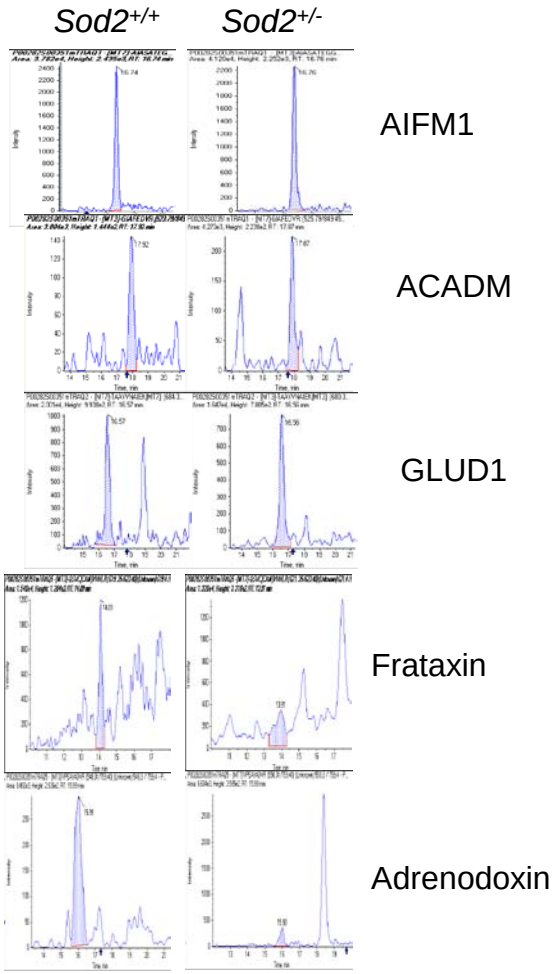

MRM

C

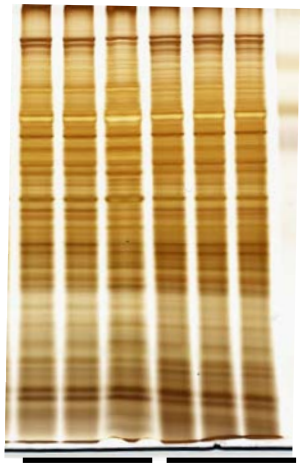

Supplementary Figure 2

A

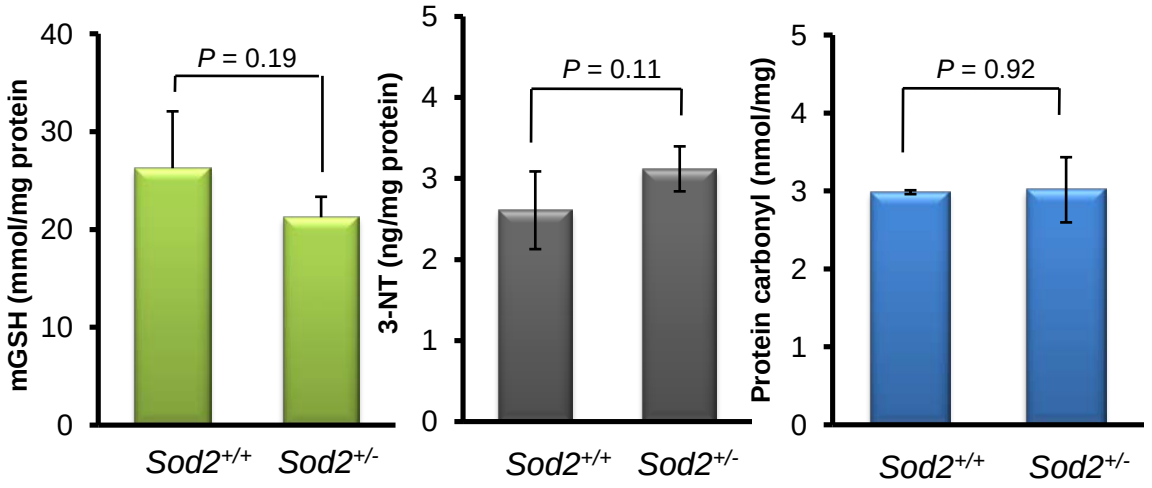

B

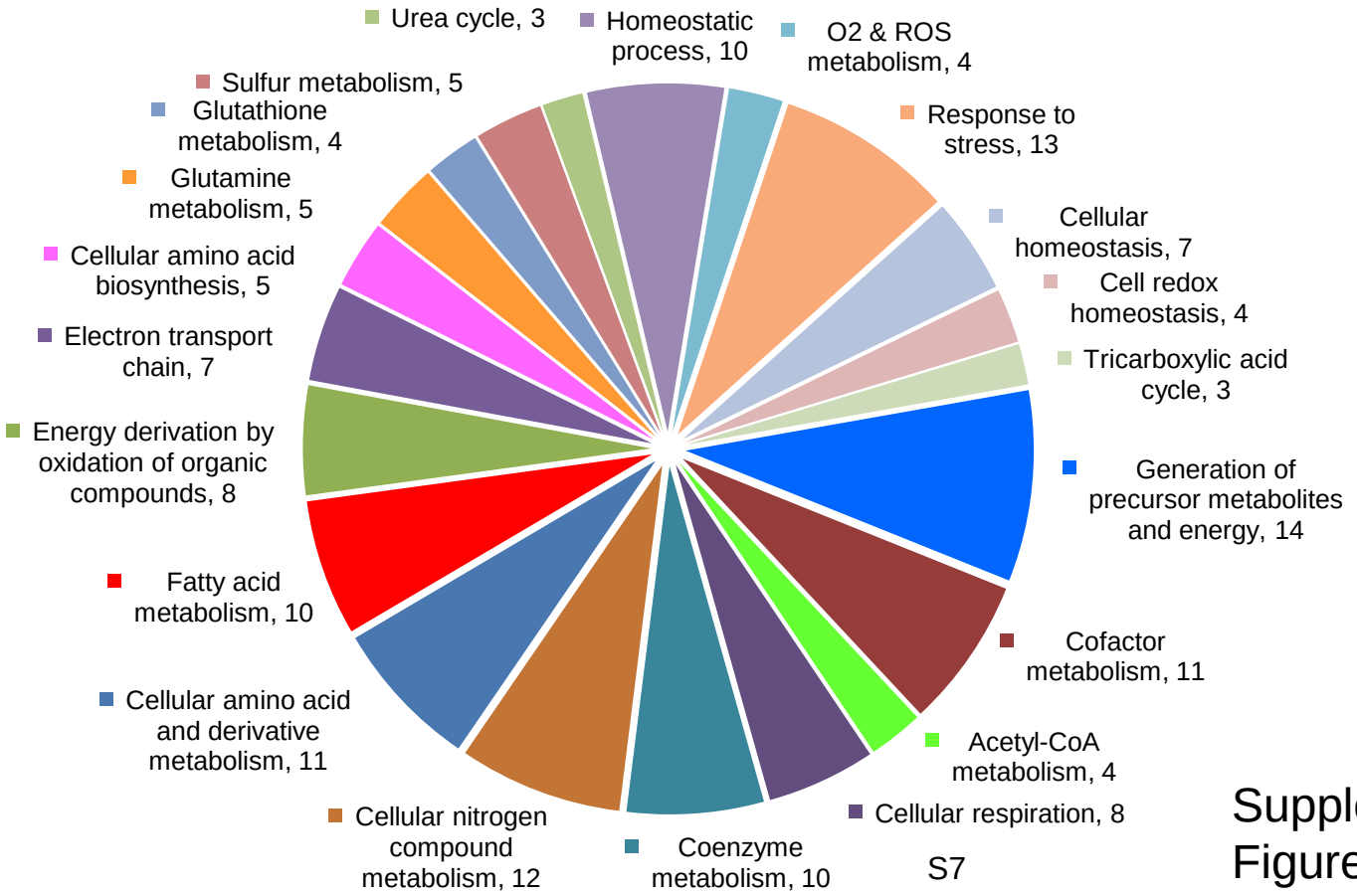

Supplementary Figure 3

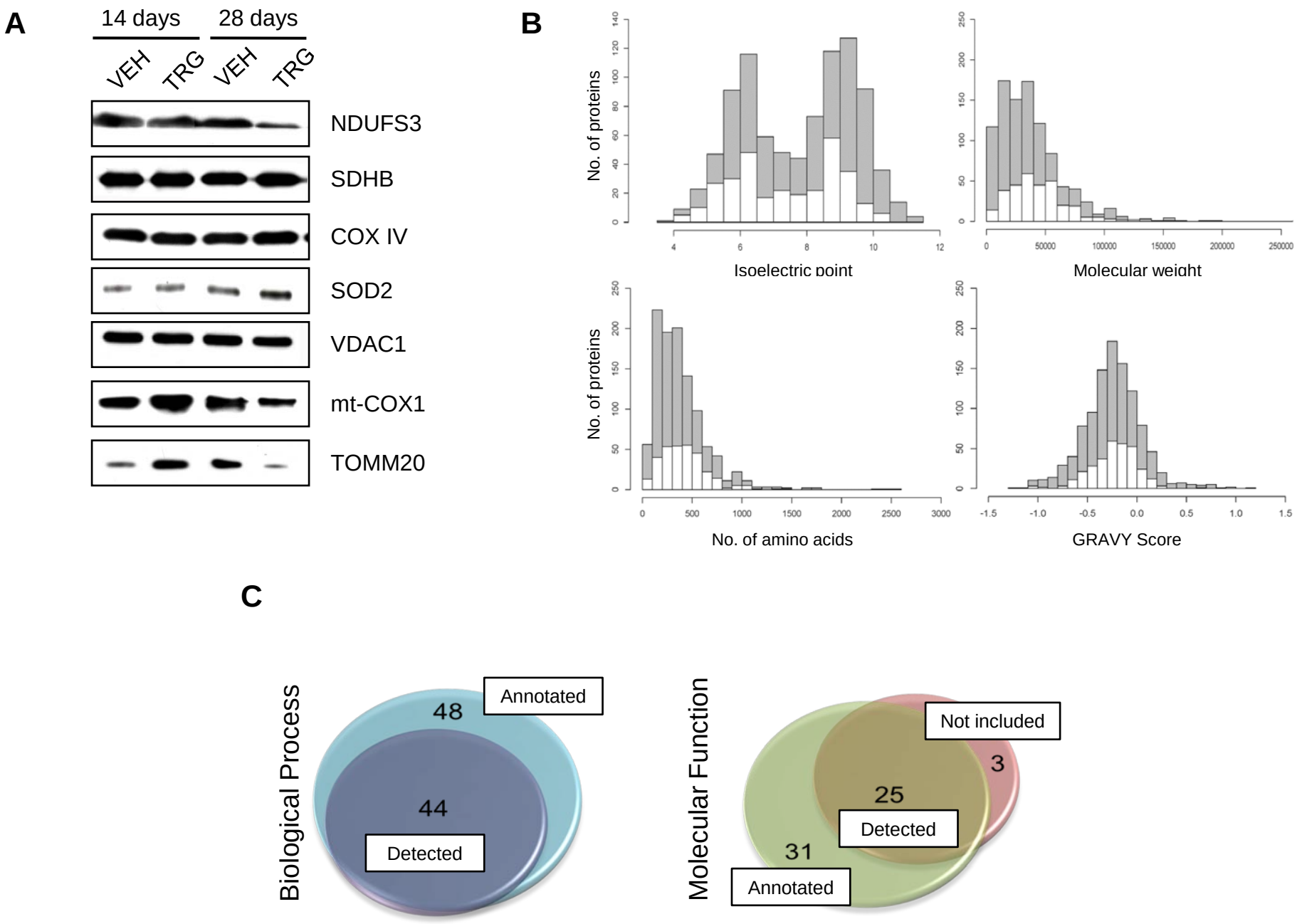

Supplementary Figure 4

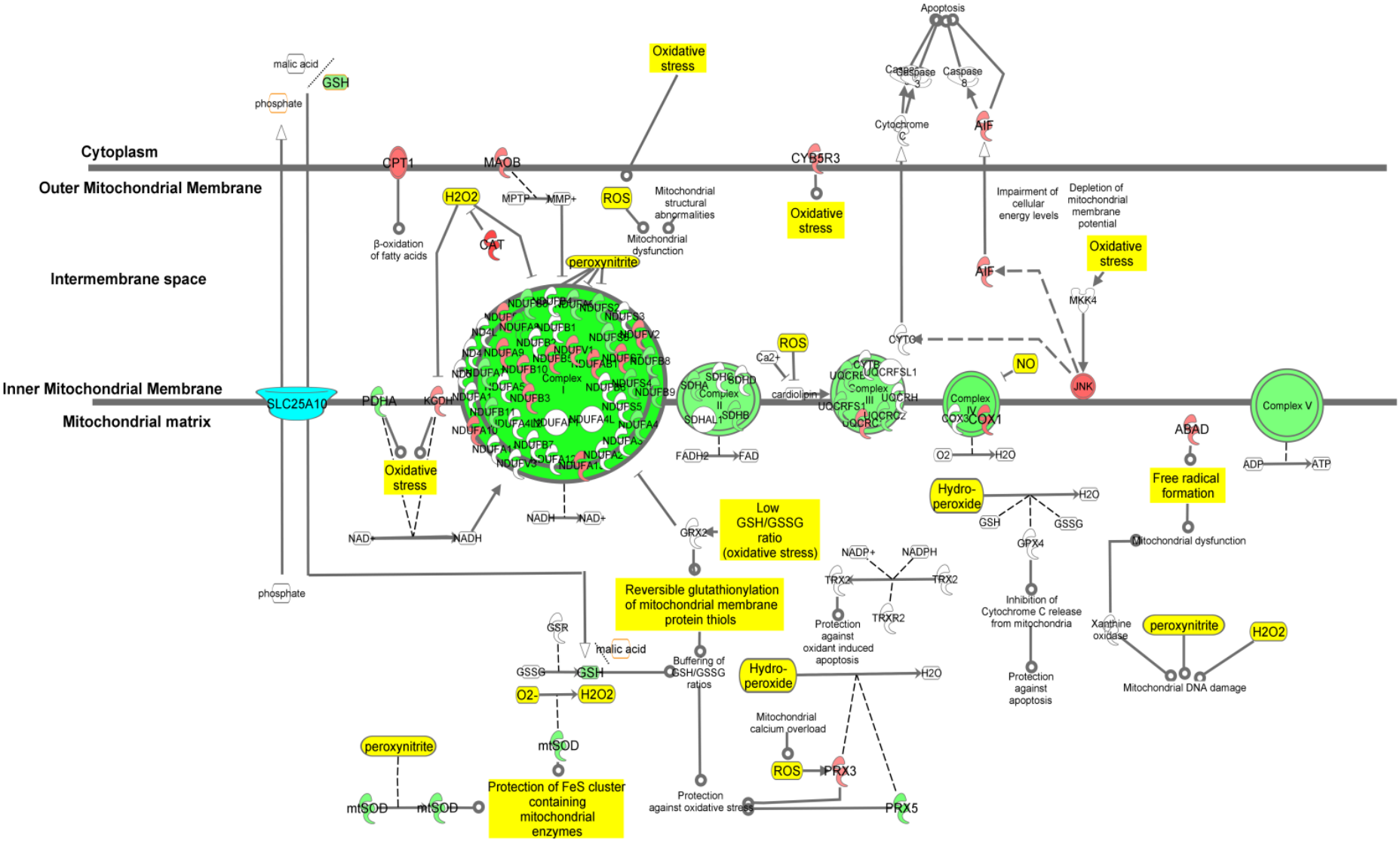

Supplementary Figure 5

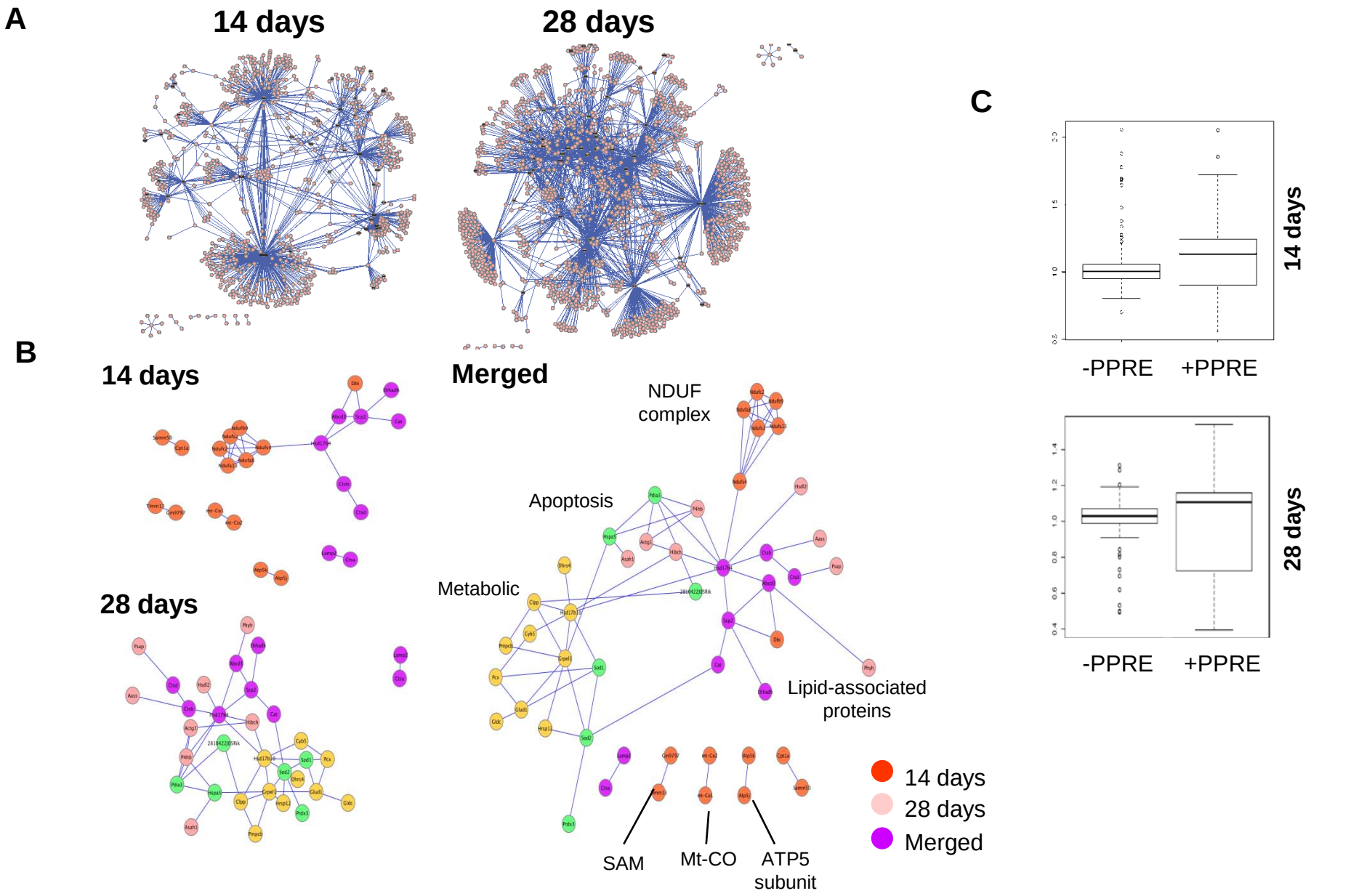

Supplementary Figure 6

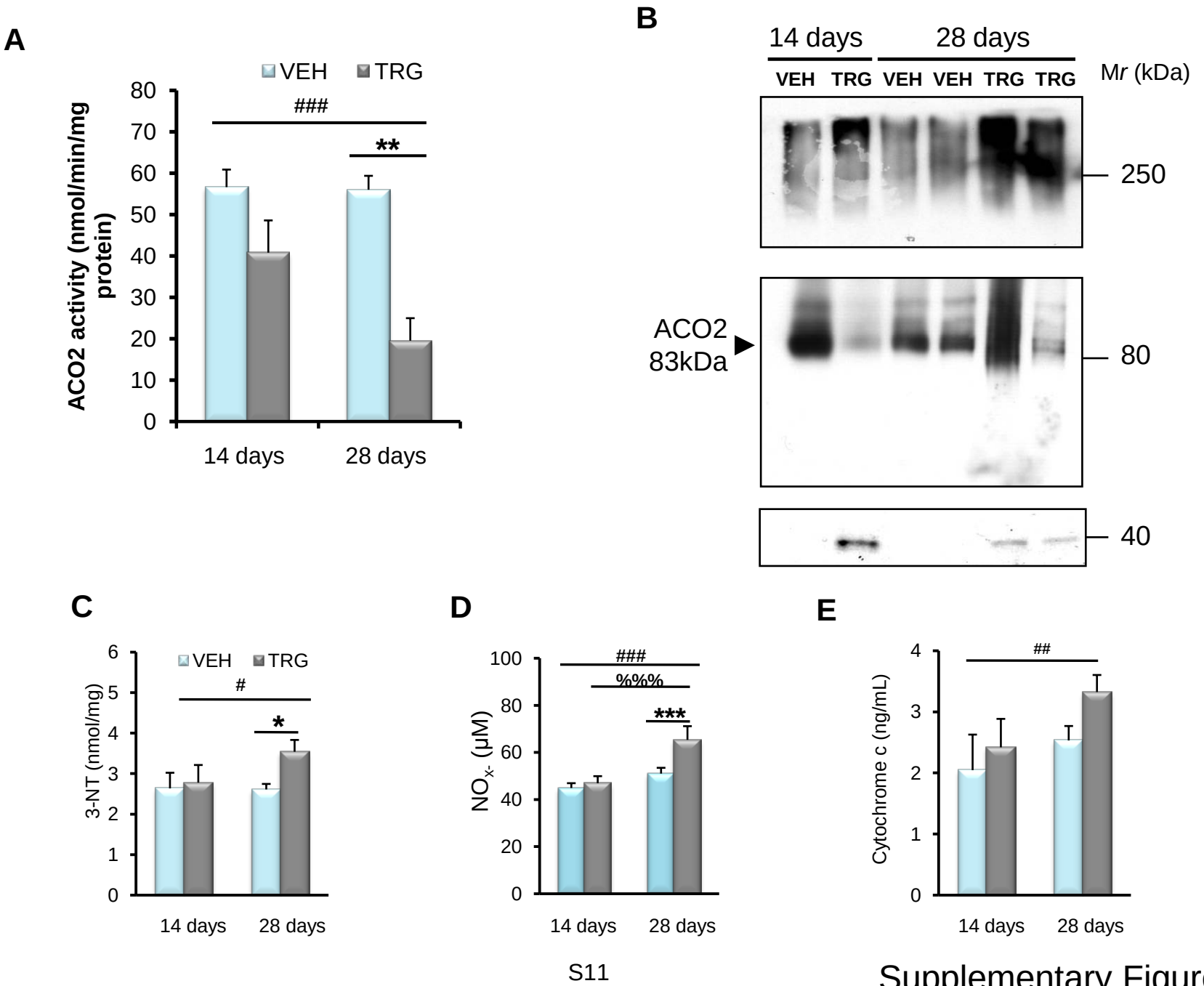

Supplementary Figure 7